Additive Strategies to Mitigate Humidity Interference Effects on PEDOT:PSS Sensors for Ammonia Detection

Ajay Beniwal, Priyanka Ganguly, Gaurav Khandelwal, Rahul Gond, Brajesh Rawat and Chong Li

***Abstract*—Development of precise and accurate ammonia sensors suitable for healthcare (point-of-care devices) and environmental monitoring is imperative and absolute necessity. However, a persistent challenge in the gas sensor technology is sensitivity degradation due to humidity interference. To address this challenge, this study presents a screen-printed, flexible, and disposable sensor based on poly(3,4-ethylenedioxythiophene): poly(styrenesulfonate) (PEDOT:PSS) mixed with additives having reduced humidity interference tailored for ammonia (NH_3) gas detection. Polar solvents such as ethylene glycol (EG), dimethylformamide (DMF) and dimethyl sulfoxide (DMSO) are used as additives with the base material PEDOT:PSS. Enhanced hydrophobicity is confirmed via contact angle measurements. Current-voltage (I-V) characteristic assessments reveal a linear ohmic behaviour, emphasising the heightened conductivity of the samples with additives compared to the PEDOT:PSS sensor. When assessing the humidity response, the DMF modified PEDOT:PSS sensor exhibited minimal % response, registering only 37.01% at 90% humidity. This was a marked improvement over the pristine PEDOT:PSS sensor, which recorded 118.5% at the same humidity level, and outperformed other additive variants. Regarding ammonia detection, the PEDOT:PSS/DMF sensor demonstrated an experimental detection ability up to 0.1 ppm with 0.91 % response and outperformed the ammonia sensing ability of pristine PEDOT:PSS. Effect of relative humidity (~5 %RH to 80 %RH) on ammonia gas sensing performance of PEDOT:PSS/DMF sensor is also conducted and compared with pristine PEDOT:PSS. The increment in sensor conductivity with rising ammonia concentrations is theorized due to the charge transfer, where ammonia's lone pair of electrons interacts with the covalent backbone of PEDOT:PSS, suggesting a plausible sensing mechanism.**

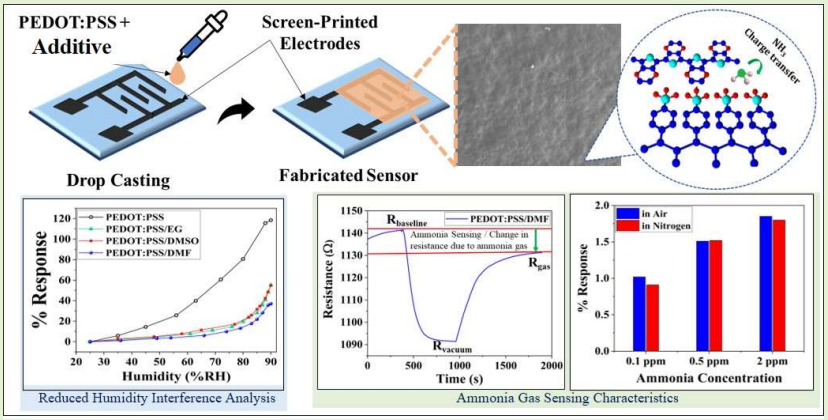

***Index Terms*— Ammonia detection, additive strategies, Eco-friendly sensor, Humidity interference, PEDOT:PSS**

I. Introduction

As urbanisation and industrialisation continue to expand, there is an increasing necessity to monitor levels of harmful gases like carbon monoxide (CO), nitrogen oxides (NO and NO_2), ammonia (NH_3), hydrogen sulfide (H_2S), methane (CH_4) ethane (C_2H_6) etc.[1-10] This monitoring ensures the safety and well-being of individuals and helps in maintaining a healthier environment amidst the growing challenges posed by urban and industrial activities. Ammonia, a key contributor amongst different air pollutants is generated through multiple sources such as industrial discharge, degradation of organic matter and from vehicular emissions.[8, 11, 12] Moreover, NH_3 is one of the key ingredients for fertilisers, fabric dye, cosmetics, pesticides, paper, plastics, explosives, and pharmaceuticals[8, 13]. However, the exposure to ammonia

This work is supported by the UK Research and Innovation (UKRI) - Engineering and Physical Sciences Research Council (EPSRC) under UKRI Postdoctoral Fellowships Guarantee scheme for Marie Sklodowska-Curie Actions (MSCA) Postdoctoral Fellowship DETECT (EP/X027791/1). This work is also supported with SERB Start-up Grant (SRG/2020/0007111), Department of Science and Technology, India.

A. Beniwal, G. Khandelwal, and C. Li are with the James Watt School of Engineering, University of Glasgow, G12 8QQ, Glasgow, UK.
P. Ganguly is with School of Human Sciences, London Metropolitan University, N7 8DB, UK.
R. Gond and B. Rawat are with the Department Electrical Engineering, Indian Institute of Technology Ropar, Rupnagar, Punjab, 140001, India. (Corresponding author: Ajay Beniwal; e-mail: Ajay.Beniwal@glasgow.ac.uk).

causes skin, eye, respiratory irritation and even airway inflammation.[14, 15] Based on American Conference of Governmental Industrial Hygienists (ACGIH) guidelines, a permissible exposure limit (PEL) of NH_3 to human beings is 25 ppm for 8 hours and 35 ppm for maximum exposure time of 15 minutes.[16] Beyond its environmental detection applications, ammonia serves as a critical biomarker for identifying renal (kidney) disease.[17-19] This is because the presence of exhaled ammonia in breath samples (~0.5 ppm for healthy individuals and higher in patients with chronic kidney disease stage 1/2/3/4/5) can provide insights into various stages of renal diseases.[20-22] Hence, ensuring precise and accurate monitoring of exhaled ammonia levels becomes imperative, ensuring its dependable and efficient use within the healthcare sector. Furthermore, monitoring NH_3 at lower levels i.e. lower ppm to ppb range, specifically in humid environment (e.g. breath analyser) is a challenging aspect due to influence of humidity on gas sensing and therefore requires the need for sensors capable to detect ammonia even at low concentrations under such conditions.[23]

There are several reports on ammonia sensors fabricated using different materials e.g. metal oxides, conducting polymers, composite materials, carbon nanomaterials etc. The reported works are structured for detection of various ammonia concentrations under different conditions.[24-30] However, effective applicability of ammonia sensors specifically in healthcare sector demands various selections measures including flexibility, suitable substrate material, biocompatibility and fabrication techniques.[31, 32] There are reported background studies on flexible ammonia sensors including a paper-based flexible ammonia sensor fabricated using inkjet technique, with silver functionalised poly(m-aminobenzene sulfonic acid) and single-walled carbon nanotubes (SWNT-PABS). The sensor displayed a quick sensing within a range of 10 ppm to 250 ppm.[33] In a related study, the researchers detailed the creation of a paper-based ammonia sensor utilising reduced graphene oxide (rGO). The synthesis of rGO was achieved using the Hummer's method, after which it was coated on a 3-inch Whatman filter paper using vacuum filtration technique. Aluminum electrodes were subsequently deposited onto the filter paper using a thermal evaporation technique. The device was effective for detecting ammonia over a wide range of concentration, with a detection limit as low as 0.43 ppm.[34] The use of conductive polymer such as PANI for ammonia sensing was also reported. The in-situ polymerisation technique was opted to deposit PANI on the surface of polyethylene terephthalate (PET) substrate with thickness of 20 µm. The fabricated sensor at room temperature was sensitive across a broad concentration range of 5 ppm to 1000 ppm, with a limit of detection measured at 5 ppm.[35] Similarly, various studies are reported for ammonia detection.[36-39] However, the use of complicated fabrication methodologies poses its own set of challenges. Also, developing sensors based on metal oxides or polymers, non-environmentally friendly substrates challenge the expansion of sustainable devices. Furthermore, the increasing volume of electronic waste combined with the rising demand for handheld, portable, and environmentally friendly sensors underscore the necessity for flexible, disposable, and sustainable sensing devices.

Along with this, fabricating an ammonia sensor that operates effectively in humid environments or within breath analysers is crucial. As humidity or water vapor is an omnipresent climatic factor either considering ambient environment or human breath.[40] Humidity presents a massive challenge as an interference element to analytes of interest in most of the gas sensors working in ppb or ppm range.[41] Hence, elimination of humidity interference is critically important for proper functioning of the gas sensors towards target analytes.[42] There are limited studies on reducing the humidity interference on gas sensing.[43-45] However, reported methods are complex involving multi-step procedures (e.g. additional layer coating of CeO_2[43], SnS_2[44]) using expensive techniques like electron-beam evaporation[43], hydrothermal route.[44] Further, most of the additional layer coatings are based on nanomaterials or nanohybrids like CeO_2 which have negative impact on the environment.[46] Therefore, an one-step eco-friendly approach is highly desirable for developing a precise and sustainable sensor suitable for gas sensing in humid environment.

The present work reports the fabrication of a disposable paper based flexible screen-printed sensor using graphene carbon ink and PEDOT:PSS as sensing material. Humidity is one of the crucial factors that affect the performance of gas sensors to detect analytes at lower concentrations like sub-ppm to ppb level. Hence, it becomes imperative to tackle this factor head on by reducing the humidity interference and thereby improving the sensitivity of the gas sensors. Therefore, the outcomes of this paper are structured as follows:

- The surface of the sensor is modified with polar solvents such as ethylene glycol (EG), dimethylformamide (DMF) and dimethyl sulfoxide (DMSO) with PEDOT:PSS as base material.
- The effect of doping/additives on conductivity of PEDOT:PSS has been reported extensively.[47, 48] However, in the present work the samples with different additives are studied for reducing the humidity interreference on ammonia sensing properties.
- The present work proposes an in-situ/one-step additive based facile and viable solution for mitigating the humidity interference to develop a precise, flexible, highly suitable, and sustainable ammonia sensor.

The originality of the work exists in proposing an in-situ additive based facile and viable solution for mitigating the humidity interference along with presenting the enhanced ammonia sensing characteristics of the flexible, and sustainable sensor as a proof of concept.

II. Materials and Methods

A. Materials

Graphene-carbon ink (C2171023D1:Graphene Carbon Ink:BG04 from Sun Chemical), along with a matt paper substrate (double sided photopaper) was utilised in this study. Chemicals including ethylene glycol (EG), dimethylformamide (DMF) and dimethyl sulfoxide (DMSO) were sourced from Sigma Aldrich, while PEDOT:PSS (PH 1000) was obtained from Ossila.

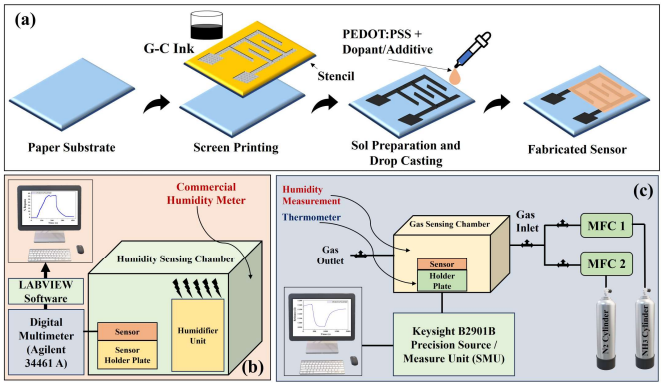

Fig. 1. Schematic illustrations of (a) sensor fabrication process, (b) humidity sensing test set-up within a humidity sensing chamber and (c) ammonia gas sensing test set-up.

B. Sensor fabrication and characterisation

Fig. 1(a) displays a detailed step of the sensor fabrication. The sensors with an interdigitated electrode (IDE) structure based on graphene-carbon ink were developed on a paper substrate. This IDE structure was fabricated using the screen-printing technique with the Screen Stencil Printer C920 from AUREL Automation. Subsequently, the printed sensors were heat treated at 60°C for 1 hour to remove the residue solvent. Further, contacts for 2-wire resistance measurements were established for device characterisation.

Additive molecules, including DMF, DMSO, and EG, were individually introduced into the PEDOT:PSS solution. The mixtures were stirred at 200 rpm for 30 minutes to achieve uniform dispersion. Subsequently, 40 µL of the dispersed solution was individually drop-casted onto the surface of the IDE printed on a paper substrate and allowed to dry overnight at 40 °C. After conducting trial-and-error experiments, the optimal concentration of additives was determined to be 5% v/v. The humidity sensing capabilities of the PEDOT:PSS sensor modified with different additives were evaluated across various volume percentages, with 5% v/v being identified as the most effective concentration for all three additives. The following steps were followed to fabricate sensors with the mixture of two additives simultaneously. A 5% v/v solution of PEDOT:PSS/DMF and a 5% v/v solution of PEDOT:PSS/EG were mixed in equal volumes and stir for 30 minutes at 200 rpm. Subsequently, 40 µL of this dispersed solution was drop-casted onto the surface of the IDE and allowed to dry overnight at 40°C to prepare PEDOT:PSS/DMF/EG sensor. Similarly, the PEDOT:PSS/DMF/DMSO solution was prepared by directly mixing equal volumes of PEDOT:PSS/DMF and PEDOT:PSS/DMSO. Moreover, the instrument information is discussed in Supporting Note 1.

C. Humidity and gas sensing set-up

The sensors' humidity sensing characteristics were monitored by placing the sensors within a custom-built humidity sensing chamber, as shown in Fig. 1(b). The information about the humidity chamber can be found in our prior work.[49] Further, an environment-controlled chamber was utilised to characterise the sensor towards ammonia detection as illustrated in Fig. 1(c). The details about humidity and gas sensing set-up are provided in Supporting Note 2.

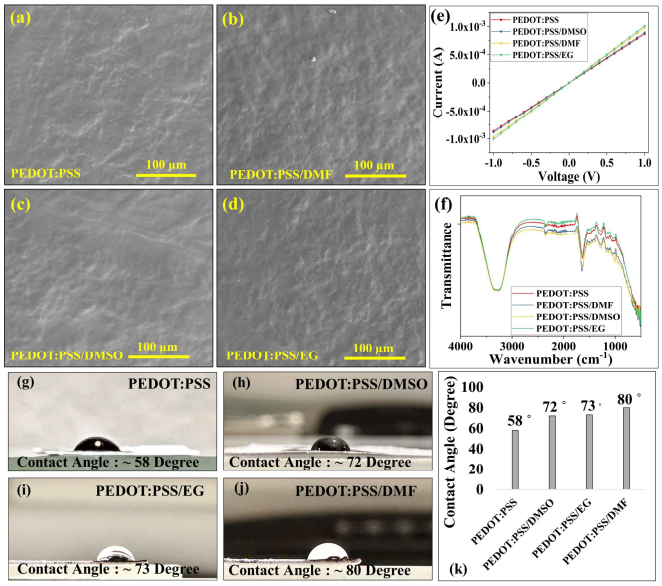

Fig. 2. SEM images of the (a) pristine PEDOT:PSS (b) PEDOT:PSS/DMF (c) PEDOT:PSS/DMSO and (d) PEDOT:PSS/EG at 100 µm scales. (e) I-V characteristics comparison and analysis. (f) FTIR analysis. Contact angle measurements for (g) pristine PEDOT:PSS; (h) PEDOT:PSS/DMSO; (i) PEDOT:PSS/EG; (j) PEDOT:PSS/DMF. (k) Comparative analysis of the obtained contact angles.

Moreover, the % response value is calculated using the following equation:

$$\%\text{Response} = \frac{\Delta R}{R_B} \times 100 \qquad \text{Eq. 1}$$

where, $\Delta R = |R_A - R_B|$; R_A is resistance at a specified humidity level or ammonia concentration; R_B is the baseline resistance.

III. Result and Discussion

A. Material and electrical characterisations

Surface morphology of the PEDOT:PSS sensor with additives are displayed in Fig. 2. The FE-SEM images of the PEDOT:PSS and PEDOT:PSS with DMF, DMSO and EG, respectively are shown in Fig. 2(a-d). The FE-SEM images confirm that there is no significant change in the morphology of PEDOT:PSS samples with additives. Fig. 2(e) shows the I-V characteristics of PEDOT: PSS and PEDOT:PSS modified with DMF, DMSO and EG having ohmic behaviour i.e. current increases linearly with voltage. The PEDOT:PSS/DMSO showed resistance close to pristine PEDOT:PSS while PEDOT:PSS/EG is the most conducting sample with least resistance value. The polar solvents like DMSO, DMF and EG exhibit high dielectric constant and are well reported to improve the conductivity of PEDOT: PSS.[47, 48] The increase in conductivity is attributed to different reasons including removal of excessive PSS, shortening of π-π stacking distance and improved sample crystallinity. Fig. 2(f) shows the FTIR spectra of PEDOT:PSS, PEDOT:PSS/DMF, PEDOT:PSS/DMSO and PEDOT:PS/EG. The peaks at 1646 cm^{-1} and 1274 cm^{-1} are related to the thiophene ring stretching vibrations. The peaks at 1040 cm^{-1} and 3291 cm^{-1} are attributed to S=O symmetrical stretching in PSS and –OH group, respectively. The increase in peak intensity with additives can be ascribed to the improved crystallinity. This displays the successful insertion of polar molecules in PEDOT:PSS samples. Fig. 2 (g-j) shows the

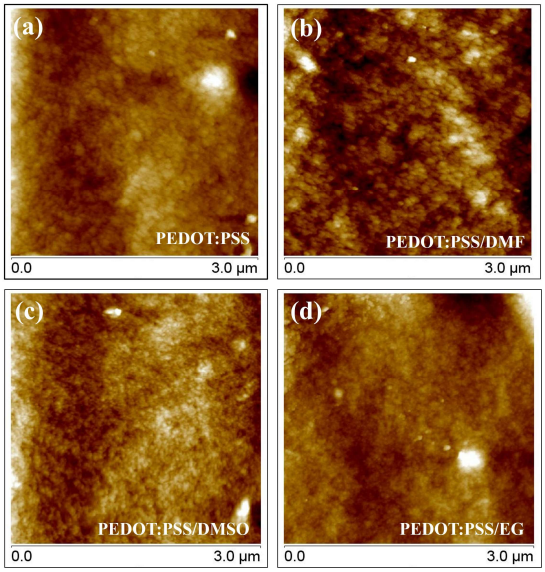

Fig. 3. AFM images of the (a) pristine PEDOT:PSS (b) PEDOT:PSS/DMF (c) PEDOT:PSS/DMSO and (d) PEDOT:PSS/EG at 3 µm scales.

contact angle images of PEDOT: PSS and PEDOT: PSS with additives and Fig. 2(k) summarises contact angles of all samples. All the samples with additives show higher contact angle than the pristine PEDOT:PSS sample (58˚). The PEDOT:PSS/DMF exhibit the highest contact angle of 80˚. The contact angle of DMSO and EG samples lies close to each other with a value of 72˚ and 73˚, respectively. This shows the increased hydrophobicity of the samples with additives compared to pristine sample as lower the contact angle as compared to 90˚, higher will be its hydrophilicity.[50-52]

Furthermore, atomic force microscopy (AFM) analysis was also carried out to examine the surface topography of the pristine PEDOT:PSS and PEDOT:PSS samples with additives DMF, DMSO and EG, as shown in the Fig. 3 (a-d). AFM results suggest a minor elongation of the grains in PEDOT:PSS samples with additives as compared to pristine sample. This minor structural elongation (due to strong affinity of additives toward PSS) leads to conductivity enhancement in PEDOT:PSS samples with additives, which is in well agreement with the background studies. [53, 54]

B. Humidity sensing performance analysis

The PEDOT:PSS mixed with additives (PEDOT:PSS/EG, PEDOT:PSS/DMSO and PEDOT:PSS/DMF) were initially investigated for humidity sensing only. The sensing characteristics of the pristine PEDOT:PSS-based humidity sensor were reported in our prior work.[55] The humidity sensing performance of the sensors with additives has been systematically investigated for a range between 25 % and 90 % RH and the results are shown in Fig. 4. The dynamic humidity sensing characteristics of the PEDOT:PSS/EG sensor in the range of 25-90 %RH are depicted in Fig. 4(a). The dynamic responses evaluated at intermediate humidity levels within the range of 25-90 %RH are presented in the Fig. 4(b).

The results reveal a significant reduction in humidity interference for EG added PEDOT:PSS, with a humidity sensing response of 55.47 % at 90 % RH, compared to the

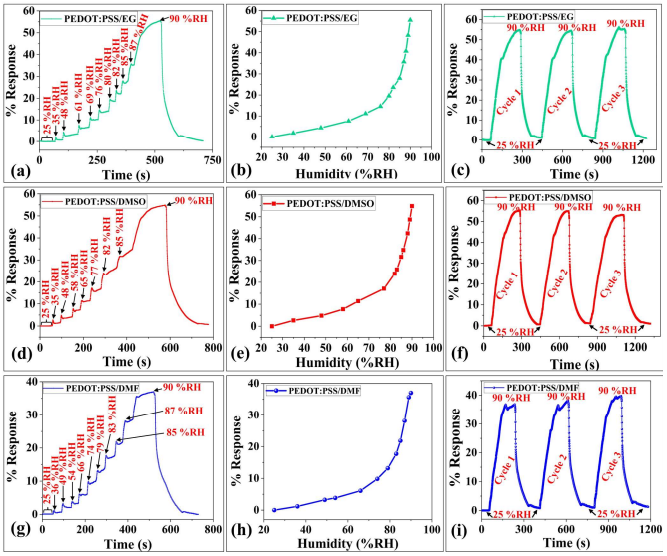

Fig. 4. Humidity sensing characteristics in range 25-90 %RH of the (a-c) PEDOT:PSS/EG sensor: (a) dynamic humidity sensing characteristics (b) % response vs humidity graph (c) 3-cyclic repeatability analysis; (d-f) PEDOT:PSS/DMSO sensor: (d) dynamic humidity sensing characteristics (e) % response vs humidity graph (f) 3-cyclic repeatability analysis; (g-i) PEDOT:PSS/DMF sensor: (g) dynamic humidity sensing characteristics (h) % response vs humidity graph (i) 3-cyclic repeatability analysis.

pristine PEDOT:PSS with a humidity sensing response of 118.5 % at 90 %RH.[55] Moreover, the repeatability of the PEDOT:PSS/EG sensor under cyclic humidity exposures was examined via a 3-cyclic repeatability test within the range of 25-90 % RH and the results are shown in Fig. 4(c). The results clearly show good repeatability indicating the sensor's suitability for repeated measurements. Similarly, the dynamic humidity sensing characteristics of the PEDOT:PSS/DMSO sensor were also examined and results are depicted in Fig. 4(d). The dynamic % responses evaluated at intermediate humidity levels (35 to 90 %RH) are perceived to be in range 2.66 % to 54.84 % as represented in Fig. 4(e). The results confirmed a significant reduction in humidity interference in PEDOT:PSS/DMSO compared to pristine PEDOT:PSS. However, the performance is comparable to PEDOT:PSS/EG when evaluated at 90 %RH. The repeatability characteristics were also examined and shown in Fig. 4(f).

Similarly, the dynamic responses were evaluated for the PEDOT:PSS/DMF sensor in the range between 25-90 %RH, as depicted in Fig. 4(g). The % responses at intermediate humidity levels i.e., 36 %RH to 90 %RH are observed to be in range 1.18 % to 37.01 % as shown in Fig. 4(h). The results clearly indicate that the humidity sensing performance is least in the PEDOT:PSS/DMF sensor compared to the previous cases (i.e., PEDOT:PSS/EG, PEDOT:PSS/DMSO and pristine PEDOT:PSS sensors). The possible reason for the lower humidity performance in the PEDOT:PSS/DFM-based sensor could be explained based on the contact angle measurement study. The deviation in the contact angle measurement (58˚ to 80˚) post-additive addition was highest in this case compared to the pristine sensor and other additive cases. This deviation (increased contact angle) indicates the movement of the sensing layer from hydrophilic to less hydrophilic i.e., the hydrophobic zone. Hydrophilicity is considered crucial for humidity sensors

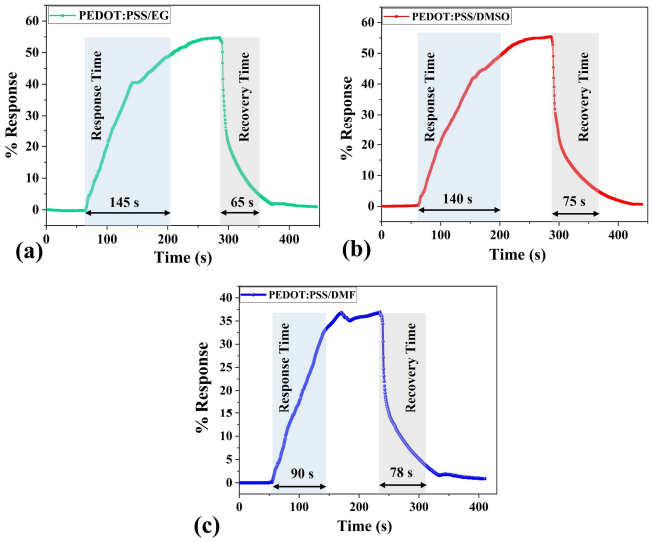

Fig. 5. Response and recovery time analysis of (a) PEDOT:PSS/EG sensor (b) PEDOT:PSS/DMSO sensor and (c) PEDOT:PSS/DMF sensor towards humidity sensing in range 25-90 %RH..

due to its significant impact on sensing properties.[49] Therefore, the promising results of reduced humidity interference in the PEDOT:PSS/DMF sensors, compared to other additives and pristine sensors, are well supported by material characterisation. Humidity or water vapor is an omnipresent climatic factor in ambient environments or human breath.[40] It poses a significant challenge as an interference element to analytes of interest in gas sensors operating at ppb or ppm levels.[41] Hence, eliminating humidity interference is critically important for the proper functioning of gas sensors towards target analytes.[42] Therefore, the present study, specifically the PEDOT:PSS/DMF sensor, proposes a single-step (in-situ additive-based), facile, and viable solution to mitigate humidity interference to develop precise and highly suitable sensors for gas sensing applications. Moreover, the repeatability study of the PEDOT:PSS/DMF sensor was examined through a 3-cyclic repeatability analysis in the range of 25-90 %RH as shown in Fig. 4(i). The results unequivocally demonstrate the sensor's capability for consistent and repeated measurements. Furthermore, the change in resistance behaviour (increase in resistance with humidity) of the PEDOT:PSS/EG, PEDOT:PSS/DMSO, and PEDOT:PSS/DMF sensors plotted using the actually measured sensor resistance values towards humidity in range 25-90 %RH is shown in Supplementary Fig. S1.

The response and recovery times of the fabricated sensors were assessed for humidity detection within the 25-90% RH range, as illustrated in Fig. 5. The response and recovery times are analysed as the duration for the sensor to reach 90 % of the response value during the response period and return back 10 % during the recovery phase.[56] The response and recovery times for PEDOT:PSS/EG are observed to be 145 s and 65 s, respectively, as shown in Fig. 5 (a). In case of PEDOT:PSS/DMSO (Fig. 5b) and PEDOT:PSS/DMF (Fig. 5c), the response/recovery durations were found to be 140 s / 75 s and 90 s / 78 s, respectively. The response/recovery times for the sensors with additives are found sluggish compared to the response (70 s) and recovery (30 s) times of the pristine

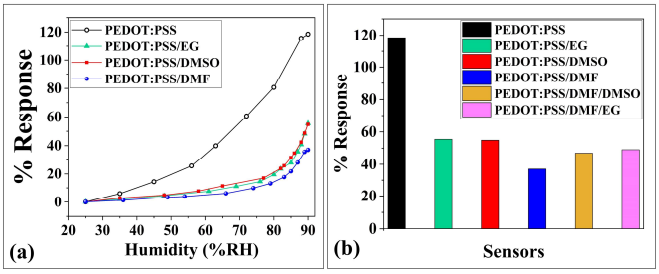

Fig. 6. (a) Comparative analysis of the humidity sensing performance of the PEDOT:PSS/EG, PEDOT:PSS/DMSO and PEDOT:PSS/DMF with PEDOT:PSS in the range of 25-90 %RH. (b) Humidity sensing performance of the PEDOT:PSS, PEDOT:PSS/EG, PEDOT:PSS/DMSO, PEDOT:PSS/DMF, PEDOT:PSS/DMF/DMSO and PEDOT:PSS/DMF/EG sensors at 90 %RH.

PEDOT:PSS humidity sensor as reported in our previous work.[55] Hence, the results indicate that, in addition to a decline in humidity sensing capabilities of the sensors with additives, there is also a noticeable delay in their response and recovery times. This characteristic makes them suitable for addressing issues related to humidity interference.

Furthermore, a comparative analysis of the humidity sensing performance among the PEDOT:PSS sensors with additives (PEDOT:PSS/EG, PEDOT:PSS/DMSO and PEDOT:PSS/DMF) and pristine PEDOT:PSS sensor is displayed in Fig. 6 (a). The comparison is concluded at discreate humidity levels within the range of 25-90 %RH. The % responses towards humidity sensing (at 90 %RH) in PEDOT:PSS/EG (55.47 %), PEDOT:PSS/DMSO (54.84 %) and PEDOT:PSS/DMF (37.01 %) sensors have been reduced to ~ 47 %, ~ 46 % and ~ 31 % compared to the % response observed for the pristine PEDOT:PSS sensor (118.5 %). Notably, the PEDOT:PSS/DMF exhibited the maximum reduction of ~ 69 % in humidity sensing, making it the most effective in minimizing humidity interference within the considered humidity range. Moreover, the PEDOT:PSS/DMF sensor is confirmed as the most effective case after analysing other scenarios where PEDOT:PSS/DMF was further mixed with DMSO and EG as shown in Fig. 6(b). These possible combinations (mixing two additives simultaneously with PEDOT:PSS) were examined considering the reduced humidity sensing in individual PEDOT:PSS/DMSO and PEDOT:PSS/EG cases. Initially, the PEDOT:PSS/DMF/DMSO based sensor was examined in the range of 25-90 %RH and the % response was observed to be 46.92 % (lower than the individual PEDOT:PSS/DMSO sensor but higher than the individual PEDOT:PSS/DMF sensor). Subsequently, the PEDOT:PSS/DMF/EG sensor was assessed under comparable conditions, yielding a response of 49.05%. While this value is lower than that of the individual PEDOT:PSS/EG sensor, it surpasses the humidity sensing response observed with the individual PEDOT:PSS/DMF sensor.

Hence, the results consistently highlight the superior efficacy of the PEDOT:PSS/DMF sensor compared to both individual and combined additive configurations with PEDOT:PSS. This enhanced performance is particularly significant for applications where humidity interference could otherwise compromise sensing accuracy. Since the dual combinations (i.e. PEDOT:PSS/DMF/DMSO and

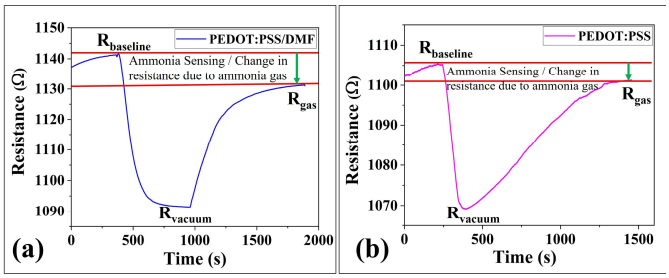

Fig. 7. (a) Change in resistance of PEDOT:PSS/DMF-based sensor at 0.1 ppm of ammonia. (c) Change in resistance of pristine PEDOT:PSS-based sensor at 0.1 ppm of ammonia.

PEDOT:PSS/DMF/EG) didn't give enhanced performance compared to the best individual case (i.e. PEDOT:PSS/DMF), the performance of the triple combination of additives (PEDOT:PSS/DMF/DMSO/EG) seems unnecessary in terms of reducing humidity interference.

Moreover, the temperature sensing behaviour of the sensors with additives was also examined to understand the impact of additives on temperature sensing properties of the sensors with additives as shown in the Fig. S2. The obtained results indicate that adding DMF, DMSO and EG into PEDOT:PSS has a minor impact on temperature sensing performance which is insignificant compared to the impact on humidity sensing properties. Detailed study is discussed in Supporting Note 3.

C. *Ammonia gas sensing performance analysis*

The ammonia sensing performance of the PEDOT:PSS/DMF sensor (in terms of change in resistance behaviour) was tested at 0.1 ppm ammonia and the results are shown in the Fig. 7(a). The baseline resistance (~ 1141.7 Ω) of the sensor is considered after the sensor was exposed to the carrier gas (N_2) at room temperature (RT) i.e., 25 °C ± 2 °C. Before exposing the sensor towards the target analyte i.e., ammonia, the sensing chamber was subjected to vacuum conditions to takeout all the ambient gases/interferences. After achieving the saturated resistance under vacuum, the sensor was exposed to target gas ammonia (NH_3) along with the nitrogen (N_2) as carrier gas through MFCs to achieve and maintain the desired concentration (0.1 ppm) of NH_3. The sensing response under ammonia exposure was examined under the similar operating conditions till the change in resistance behaviour saturated. The resistance under the target gas (i.e., NH_3 + N_2) reduced to ~ 1131.3 Ω from the baseline value of ~ 1141.7 Ω. The response and recovery time for the PEDOT:PSS/DMF sensor is observed as 60 s and 80 s, respectively. Additionally, for a comparative assessment, the response of pristine PEDOT:PSS towards 0.1 ppm ammonia concentration was also evaluated using the same method as shown in the Fig. 7(b). The resistance under the target gas (i.e., NH_3 + N_2) reduces to ~ 1101.2 Ω from the baseline resistance of ~ 1105.2 Ω which was obtained under the exposure to carrier gas (N_2) only.

The PEDOT:PSS/DMF sensor was further examined for ammonia gas sensing at room temperature (in nitrogen (N_2) and air environments as shown in Fig. 8a) owning to its superiority for mitigating the humidity interference. The % responses observed in N_2, and air environments are compared

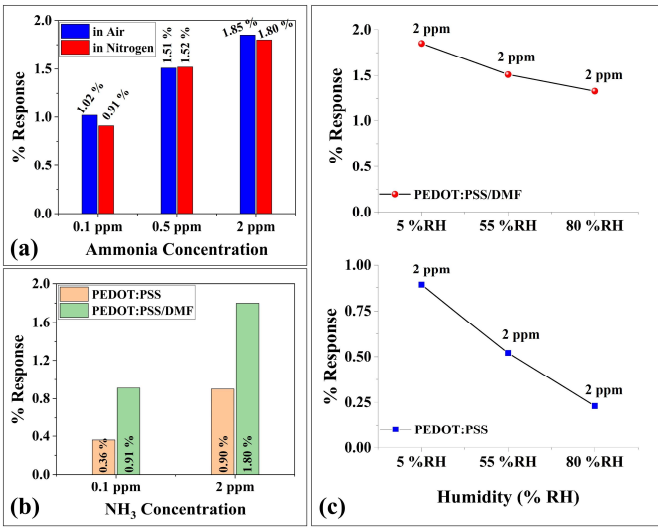

Fig. 8. Understanding the impact of DMF additive on ammonia gas sensing performance of PEDOT:PSS at room temperature in N_2 and air environment. (a) % Response vs concentration graph for PEDOT:PSS/DMF sensor at 0.1 ppm, 0.5 ppm and 2 ppm of ammonia in air and N_2 environment. (d) Comparative analysis on the sensing performance of pristine PEDOT:PSS and PEDOT:PSS/DMF sensors at 0.1 ppm and 2 ppm of ammonia. (c) Effect of relative humidity on ammonia gas sensing properties of PEDOT:PSS/DMF sensor as compared to pristine PEDOT:PSS at 2 ppm of ammonia concentration.

and represented in Fig. 8(a). The obtained results suggests that sensor's response in air environment is found to be almost similar to N_2 environment. Moreover, to assess the impact of DMF additive in gas sensing applications, the ammonia sensing characteristics (at 0.1 and 2 ppm) of the PEDOT:PSS/DMF sensor are examined and compared with the pristine PEDOT:PSS sensor as shown in the Fig. 8(b). The calculated % response for PEDOT:PSS/DMF sensor at 0.1 ppm of ammonia is 0.91 %, whereas, for pristine PEDOT:PSS sensor it is found to be 0.36 % i.e. significantly less.

Furthermore, the impact of humid conditions (~5 %RH to 80 %RH) on ammonia sensing performance of PEDOT:PSS/DMF sensor was also studied and compared with the pristine PEDOT:PSS sensor as shown in Fig. 8(c). The % response of PEDOT:PSS/DMF sensor was examined for 2 ppm of ammonia at 5 %RH, 55 %RH and 80 %RH and found to be 1.85 %, 1.51 % and 1.33 %, respectively. Herein, the % response is reduced (for 5 %RH to 80 %RH range) by 28 % whereas, the % response of pristine PEDOT:PSS sensor reduced from 0.89 % to 0.23 %, which is 74 %. This reduced sensing performance of the pristine sensor could be ascribed to the humidity interference as ammonia sensing properties are strongly influenced by humidity presence. The calculated sensitivities towards humidity variation (for a fixed ammonia concentration) for pristine PEDOT:PSS and PEDOT:PSS/DMF sensors are observed as 0.0086 %R/%RH and 0.0069 %R/%RH, respectively. The obtained results suggests that PEDOT:PSS/DMF sensor is relatively more immune to humidity, which indicates the importance of DMF additive towards reducing the humidity interference. Therefore, the obtained results evidently suggest the importance of adding DMF in PEDOT:PSS to improve ammonia gas sensing performance by reducing the humidity interference.

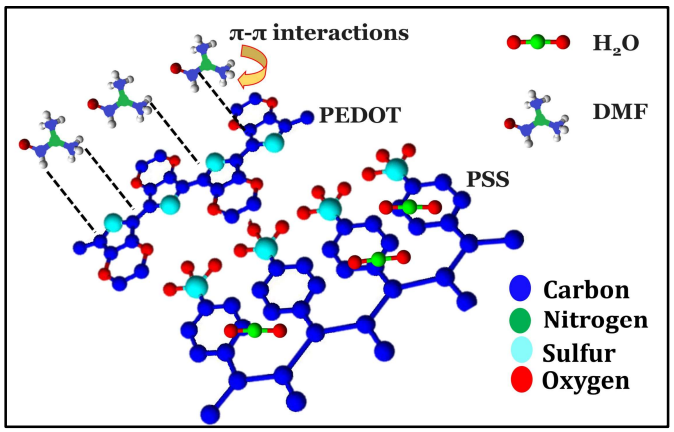

Fig. 9. Schematic depiction of the humidity sensing mechanism of PEDOT:PSS sensor with additive.

Hence, the attained results distinctly show the merits of the present work towards developing ammonia sensor which could be effectively used in humid environment or breath analysers. Along with environmental detection of ammonia,[1, 57] it is a vital biomarker for detection of renal (kidney) diseases as exhaled ammonia through breath could be used to determine different stages of renal diseases.[21, 22, 58] Therefore, precise, and accurate monitoring of exhaled ammonia level is absolute requirement for their reliable and effective utilisation in healthcare sector. Although, the developed method seems suitable and can be applied in renal diseases detection/monitoring as a futuristic application or any other application with modifications in the target detection range and other sensing characteristics.

D. Sensing mechanism

The conductive polymers, such as PEDOT:PSS, are composed of cationic short chains of PEDOT combined with the anionic, long covalent backbone of PSS. The conductivity in these polymers arises from the overlapping π orbitals along the polymer backbone. Any alteration in conductivity typically stems from disruptions in charge transfer among these overlapping π orbitals. Factors like structural irregularities such as increased intermolecular spacing or alterations in relative orientation can interrupt this charge transport. This disruption becomes particularly evident when considering sensing applications, as demonstrated in our prior research on NO_2 detection.[56] When gas molecules physiosorbed on the surface of the PEDOT:PSS, they induce structural irregularities, thereby hindering charge transport and leading to change in resistance.[47, 48, 59]

Humidity sensing mechanism: Humidity is a significant interfering factor in gas sensing applications, both in ambient conditions and in human breath, as discussed in Section 3.2. Therefore, monitoring gas analytes with sensors designed to minimise humidity interference is crucial for achieving optimal response. In our earlier work, we investigated the influence of PEDOT:PSS modified sensors for humidity applications. [55, 60] Water molecules physiosorbed on the surface, particularly in the PSS regions. The π-π stacking distance between PEDOT chains remains unchanged upon adsorption of water molecules. [61, 62] However, the distance between PEDOT and PSS molecules increases with rising humidity levels. This change affects the inter-chain hopping of electrons, leading to a decrease in resistance with increasing humidity levels. The schematic illustration of the humidity sensing mechanism of the PEDOT:PSS sensor with additive is shown in Fig. 9.

The introduction of additive molecules to modify PEDOT:PSS has shown a significant impact in minimising changes in resistance in response to increased humidity levels compared to pristine PEDOT:PSS. The PEDOT:PSS with additives introduces coulombic interactions between the charge carriers and counter ions. This interaction localises the charge carriers, resulting in ionised impurities within the structure. However, when added with polar solvents like DMF, DMSO with high dielectric constant, these coulombic interactions between PEDOT and PSS molecules are mitigated.[47, 48, 59] As a result, the conductivity of PEDOT:PSS improves. Reflected in the aforementioned results, the PEDOT:PSS samples exhibited similar increase in conductivity but the changes are not significant as the dopant ratios are relatively low.

This effect is also reflected in the altered surface properties observed in the modified sensors. The hydrophobicity of the modified sensors increases compared to the pristine ones. The addition of polar molecules strengthens π–π interactions between PEDOT chains, enhancing inter-chain transport of carriers and improving overall conductivity (Fig. 8). [63] However, in this study, the introduced dopant ratios were relatively low to observe a significant change in conductivity values. Nevertheless, while the introduction of additives may not necessarily increase conductivity values, it does help compensate for the resistance increase introduced by water molecules, as evidenced by the results shown in Fig. 6. Notably, the DMF-added PEDOT:PSS samples demonstrated optimal non-interference to humidity.

Ammonia gas sensing mechanism: With regards to ammonia sensing, the PEDOT:PSS sensor and the PEDOT:PSS/DMF sensor displayed decrease in resistance with the increase in the ammonia concentration. This decrease in the resistance was higher in case of sensor with additive as compared to pristine PEDOT:PSS. The change in resistance could be explained through different hypotheses. One possible explanation is that the interaction between the target analyte i.e., ammonia (which is an electron-donating molecule) and the PEDOT:PSS sensing layer leads to this change in resistance. [47, 48, 64, 65] The lone pair of electrons on the nitrogen atom forms a co-ordinate covalent bond with PEDOT:PSS. This bonding interaction enhances the overall charge transfer, which in turn improves the conductivity (i.e., reduces the resistance) as the ammonia concentration increases. [66, 67] Furthermore, ammonia interaction with PEDOT:PSS layer converts the core-shell structure to a linear conformation, which leads to reducing the roughness and enhances the conductivity of the PEDOT:PSS layer. [68] Moreover, The reason that the sensor with additive displayed greater response in terms of change in resistance in presence of ammonia could be explained as a combination of decreased columbic interaction between the ionic charges and the charge carriers as well as the charge transfer from ammonia to the sensor surface.[47, 48, 64, 65] Fig. 10 displays the summarised depiction of the ammonia sensing mechanism.

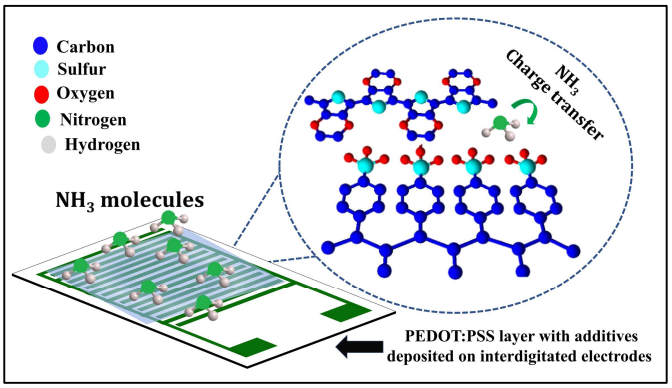

Fig. 10. Schematic depiction of the ammonia sensing mechanism of PEDOT:PSS.

Hence the results suggest that the primary mechanism facilitating NH_3 detection in the PEDOT:PSS/DMF sensor is most likely due to the direct charge transfer process. Furthermore, it is important to highlight that these sensors show limited reaction to humidity. This characteristic is particularly noteworthy because numerous polymer-based gas sensors usually function through a swelling mechanism, rendering them highly susceptible to humidity. The diminished sensitivity of the PEDOT:PSS/DMF sensor to humidity emphasises its potential benefits and appropriateness for applications where such environmental factors might otherwise create difficulties. Moreover, the PEDOT:PSS/DMF sensor displays a quick dynamic response. It nearly fully recovers to its baseline resistance within a brief span of desorption period at room temperature. This rapid recovery is especially noteworthy in situations where physisorption is more prevalent than chemisorption.[47, 48, 64, 65]

IV. Conclusion

The present study showcases the fabrication of flexible and disposable ammonia sensor which display limited reaction in the presence of humidity. Herein, the additive strategies were developed to mitigate the impact of humidity on PEDOT:PSS-based sensors for their potential applicability in ammonia sensing applications. Graphene-carbon electrodes were printed on a bio-degradable paper substrate using the screen-printing technique. The PEDOT:PSS sensing layer developed using various additives including DMF, DMSO and EG and deposited using the drop-casting method. FTIR results confirmed the presence of additives in PEDOT:PSS. FESEM and AFM analysis revealed the minor changes on the surface of the sensor with and without the additives. The increased hydrophobicity measured using contact angle measurements confirmed the limited interaction of water molecules as evident in the humidity sensing measurements with 25-90% RH. Among the sensors, the PEDOT:PSS/DMF-based sensor demonstrated superior performance in mitigating humidity interference and displayed potential applicability in ammonia sensing applications. To demonstrate the impact/advancement achieved in ammonia sensing performance by reducing the humidity interference in PEDOT:PSS/DMF sensor, the ammonia sensing characteristics (in the range of 0.1 - 2 ppm) are presented as a proof of concept. The results distinctly show the significance of developing ammonia sensor effective in humid environments such as breath analysers. The sensing mechanism was also given. Thus, this research underscores the significance of additive strategies in alleviating the challenges posed by humidity interference on PEDOT:PSS-based sensors, thereby enhancing their efficacy for gas sensing applications.

References

[1] Q. Lu, L. Huang, W. Li *et al.*, "Mixed-potential ammonia sensor using Ag decorated $FeVO_4$ sensing electrode for automobile in-situ exhaust environment monitoring," *Sensors and Actuators B: Chemical,* vol. 348, pp. 130697, 2021.

[2] Z. Xu, A. Song, F. Wang *et al.*, "Sensitive and effective imaging of carbon monoxide in living systems with a near-infrared fluorescent probe," *RSC Advances,* vol. 11, no. 51, pp. 32203-32209, 2021.

[3] S. G. Al-Kindi, R. D. Brook, S. Biswal *et al.*, "Environmental determinants of cardiovascular disease: lessons learned from air pollution," *Nature Reviews Cardiology,* vol. 17, no. 10, pp. 656-672, 2020.

[4] D. Tyagi, H. Wang, W. Huang *et al.*, "Recent advances in two-dimensional-material-based sensing technology toward health and environmental monitoring applications," *Nanoscale,* vol. 12, no. 6, pp. 3535-3559, 2020.

[5] T. Pham, G. Li, E. Bekyarova *et al.*, "MoS_2-Based Optoelectronic Gas Sensor with Sub-parts-per-billion Limit of NO_2 Gas Detection," *ACS Nano,* vol. 13, no. 3, pp. 3196-3205, 2019.

[6] F. I. M. Ali, F. Awwad, Y. E. Greish *et al.*, "Hydrogen Sulfide (H_2S) Gas Sensor: A Review," *IEEE Sensors Journal,* vol. 19, no. 7, pp. 2394-2407, 2019.

[7] L. Yang, Z. Wang, X. Zhou *et al.*, "Synthesis of Pd-loaded mesoporous SnO_2 hollow spheres for highly sensitive and stable methane gas sensors," *RSC Advances,* vol. 8, no. 43, pp. 24268-24275, 2018.

[8] M. Wu, M. He, Q. Hu *et al.*, "Ti_3C_2 MXene-Based Sensors with High Selectivity for NH_3 Detection at Room Temperature," *ACS Sensors,* vol. 4, no. 10, pp. 2763-2770, 2019.

[9] M. R. Adib, V. V. Kondalkar, and K. Lee, "Development of Highly Sensitive Ethane Gas Sensor Based on 3D WO_3 Nanocone Structure Integrated with Low-Powered In-Plane Microheater and Temperature Sensor," *Advanced Materials Technologies,* vol. 5, no. 5, pp. 2000009, 2020.

[10] S. K. Lalwani, A. Beniwal, and Sunny, "Enhancing room temperature ethanol sensing using electrospun Ag-doped SnO_2–ZnO nanofibers," *Journal of Materials Science: Materials in Electronics,* vol. 31, no. 20, pp. 17212-17224, 2020.

[11] S. N. Behera, M. Sharma, V. P. Aneja *et al.*, "Ammonia in the atmosphere: a review on emission sources, atmospheric chemistry and deposition on terrestrial bodies," *Environmental Science and Pollution Research,* vol. 20, no. 11, pp. 8092-8131, 2013.

[12] M. Sonker, S. K. Tiwary, N. Shreyash *et al.*, "Ammonia as an alternative fuel for vehicular applications: Paving the way for adsorbed ammonia and direct ammonia fuel cells," *Journal of Cleaner Production,* vol. 376, pp. 133960, 2022.

[13] R. S. Ganesh, E. Durgadevi, M. Navaneethan *et al.*, "Tuning the selectivity of NH_3 gas sensing response using Cu-doped ZnO nanostructures," *Sensors and Actuators A: Physical,* vol. 269, pp. 331-341, 2018.

[14] M. Zhang, J. Chen, X. Mao *et al.*, "Fluorescent nonwoven fabric with synergistic dual fluorescence emission for visible and selective ammonia gas detection," *Radiation Physics and Chemistry,* vol. 201, pp. 110453, 2022.

[15] H. Wang, X. Zeng, X. Zhang *et al.*, "Ammonia exposure induces oxidative stress and inflammation by destroying the microtubule structures and the balance of solute carriers in the trachea of pigs," *Ecotoxicology and Environmental Safety,* vol. 212, pp. 111974, 2021.

[16] D. A. Khudhur, T. A. Tuan Abdullah, and N. Norazahar, "A Review of Safety Issues and Risk Assessment of Industrial Ammonia Refrigeration System," *ACS Chemical Health & Safety,* vol. 29, no. 5, pp. 394-404, 2022.

[17] J.-W. Yoon, and J.-H. Lee, "Toward breath analysis on a chip for disease diagnosis using semiconductor-based chemiresistors: recent progress and future perspectives," *Lab on a Chip,* vol. 17, no. 21, pp. 3537-3557, 2017.

[18] R. Kalidoss, S. Umapathy, and U. Rani Thirunavukkarasu, "A breathalyzer for the assessment of chronic kidney disease patients' breathprint: Breath flow dynamic simulation on the measurement chamber and experimental investigation," *Biomedical Signal Processing and Control,* vol. 70, pp. 103060, 2021.

[19] R. Kalidoss, R. Kothalam, A. Manikandan *et al.*, "Socio-economic demands and challenges for non-invasive disease diagnosis through a portable breathalyzer by the incorporation of 2D nanosheets and SMO nanocomposites," *RSC Advances,* vol. 11, no. 35, pp. 21216-21234, 2021.

[20] S. Bevc, E. Mohorko, M. Kolar *et al.*, "Measurement of breath ammonia for detection of patients with chronic kidney disease," *Clin Nephrol,* vol. 88, no. 13, pp. 14-17, 2017.

[21] L. R. Narasimhan, W. Goodman, and C. K. N. Patel, "Correlation of breath ammonia with blood urea nitrogen and creatinine during hemodialysis," *Proceedings of the National Academy of Sciences,* vol. 98, no. 8, pp. 4617-4621, 2001.

[22] M.-J. Chan, Y.-J. Li, C.-C. Wu *et al.*, "Breath Ammonia Is a Useful Biomarker Predicting Kidney Function in Chronic Kidney Disease Patients," *Biomedicines,* 8, 2020].

[23] S. Singh, J. Deb, U. Sarkar *et al.*, "MoS2/MoO3 Nanocomposite for Selective NH3 Detection in a Humid Environment," *ACS Sustainable Chemistry & Engineering,* vol. 9, no. 21, pp. 7328-7340, 2021/05/31, 2021.

[24] K. Madgula, and L. N. Shubha, "Conducting Polymer Nanocomposite-Based Gas Sensors," *Functional Nanomaterials: Advances in Gas Sensing Technologies*, S. Thomas, N. Joshi and V. K. Tomer, eds., pp. 399-431, Singapore: Springer Singapore, 2020.

[25] S. Manivannan, A. M. Saranya, B. Renganathan *et al.*, "Single-walled carbon nanotubes wrapped poly-methyl methacrylate fiber optic sensor for ammonia, ethanol and methanol vapors at room temperature," *Sensors and Actuators B: Chemical,* vol. 171-172, pp. 634-638, 2012.

[26] M. E. Meyerhoff, "Polymer membrane electrode based potentiometric ammonia gas sensor," *Analytical Chemistry,* vol. 52, no. 9, pp. 1532-1534, 1980.

[27] X. Liu, W. Zheng, R. Kumar *et al.*, "Conducting polymer-based nanostructures for gas sensors," *Coordination Chemistry Reviews,* vol. 462, pp. 214517, 2022.

[28] D. Kwak, Y. Lei, and R. Maric, "Ammonia gas sensors: A comprehensive review," *Talanta,* vol. 204, pp. 713-730, 2019.

[29] A. Beniwal, and Sunny, "SnO_2-ZnO-Fe_2O_3 tri-composite based room temperature operated dual behavior ammonia and ethanol sensor for ppb level detection," *Nanoscale,* vol. 12, no. 38, pp. 19732-19745, 2020.

[30] A. Beniwal, and Sunny, "Highly selective and sensitive O_2 plasma treated sputtered thin film sensor for sub-ppm level NH_3 detection at room temperature," *Journal of Materials Science: Materials in Electronics,* vol. 30, no. 3, pp. 3144-3155, 2019.

[31] T.-P. Huynh, and H. Haick, "Autonomous Flexible Sensors for Health Monitoring," *Advanced Materials,* vol. 30, no. 50, pp. 1802337, 2018.

[32] S. Khan, S. Ali, and A. Bermak, "Recent Developments in Printing Flexible and Wearable Sensing Electronics for Healthcare Applications," *Sensors,* 19, 2019.

[33] L. Huang, P. Jiang, D. Wang *et al.*, "A novel paper-based flexible ammonia gas sensor via silver and SWNT-PABS inkjet printing," *Sensors and Actuators B: Chemical,* vol. 197, pp. 308-313, 2014/07/05/, 2014.

[34] R. Ghosh, A. Singh, S. Santra *et al.*, "Highly sensitive large-area multi-layered graphene-based flexible ammonia sensor," *Sensors and Actuators B: Chemical,* vol. 205, pp. 67-73, 2014.

[35] L. Kumar, I. Rawal, A. Kaur *et al.*, "Flexible room temperature ammonia sensor based on polyaniline," *Sensors and Actuators B: Chemical,* vol. 240, pp. 408-416, 2017.

[36] D. Lv, W. Shen, W. Chen *et al.*, "PSS-PANI/PVDF composite based flexible NH_3 sensors with sub-ppm detection at room temperature," *Sensors and Actuators B: Chemical,* vol. 328, pp. 129085, 2021.

[37] S. Veeralingam, P. Sahatiya, and S. Badhulika, "Low cost, flexible and disposable $SnSe_2$ based photoresponsive ammonia sensor for detection of ammonia in urine samples," *Sensors and Actuators B: Chemical,* vol. 297, pp. 126725, 2019.

[38] S. Matindoust, A. Farzi, M. Baghaei Nejad *et al.*, "Ammonia gas sensor based on flexible polyaniline films for rapid detection of spoilage in protein-rich foods," *Journal of Materials Science: Materials in Electronics,* vol. 28, no. 11, pp. 7760-7768, 2017.

[39] N. Tang, C. Zhou, L. Xu *et al.*, "A Fully Integrated Wireless Flexible Ammonia Sensor Fabricated by Soft Nano-Lithography," *ACS Sensors,* vol. 4, no. 3, pp. 726-732, 2019.

[40] A. Enjin, "Humidity sensing in insects—from ecology to neural processing," *Current Opinion in Insect Science,* vol. 24, pp. 1-6, 2017.

[41] J. Yu, D. Wang, V. V. Tipparaju *et al.*, "Mitigation of Humidity Interference in Colorimetric Sensing of Gases," *ACS Sensors,* vol. 6, no. 2, pp. 303-320, 2021.

[42] X.-H. Ma, H.-Y. Li, S.-H. Kweon *et al.*, "Highly Sensitive and Selective $PbTiO_3$ Gas Sensors with Negligible Humidity Interference in Ambient Atmosphere," *ACS Applied Materials & Interfaces,* vol. 11, no. 5, pp. 5240-5246, 2019.

[43] H.-Y. Li, C.-S. Lee, D. H. Kim *et al.*, "Flexible Room-Temperature NH_3 Sensor for Ultrasensitive, Selective, and Humidity-Independent Gas Detection," *ACS Applied Materials & Interfaces,* vol. 10, no. 33, pp. 27858-27867, 2018.

[44] Y. Huang, W. Jiao, Z. Chu *et al.*, "High Sensitivity, Humidity-Independent, Flexible NO_2 and NH_3 Gas Sensors Based on SnS2 Hybrid Functional Graphene Ink," *ACS Applied Materials & Interfaces,* vol. 12, no. 1, pp. 997-1004, 2020.

[45] Y. Jung, H. G. Moon, C. Lim *et al.*, "Humidity-Tolerant Single-Stranded DNA-Functionalized Graphene Probe for Medical Applications of Exhaled Breath Analysis," *Advanced Functional Materials,* vol. 27, no. 26, pp. 1700068, 2017.

[46] Y. H. Leung, M. M. N. Yung, A. M. C. Ng *et al.*, "Toxicity of CeO_2 nanoparticles – The effect of nanoparticle properties," *Journal of Photochemistry and Photobiology B: Biology,* vol. 145, pp. 48-59, 2015.

[47] J. Y. Kim, J. H. Jung, D. E. Lee *et al.*, "Enhancement of electrical conductivity of poly(3,4-ethylenedioxythiophene)/poly(4-styrenesulfonate) by a change of solvents," *Synthetic Metals,* vol. 126, no. 2, pp. 311-316, 2002.

[48] N. A. A. Shahrim, Z. Ahmad, A. Wong Azman *et al.*, "Mechanisms for doped PEDOT:PSS electrical conductivity improvement," *Materials Advances,* vol. 2, no. 22, pp. 7118-7138, 2021.

[49] A. Beniwal, P. Ganguly, A. K. Aliyana *et al.*, "Screen-printed Graphene-carbon Ink based Disposable Humidity Sensor with Wireless Communication," *Sensors and Actuators B: Chemical*, 2022.

[50] X. Feng, L. Feng, M. Jin *et al.*, "Reversible super-hydrophobicity to super-hydrophilicity transition of aligned ZnO nanorod films," *Journal of the American Chemical Society,* vol. 126, no. 1, pp. 62-63, 2004.

[51] Z. Duan, Y. Jiang, M. Yan *et al.*, "Facile, flexible, cost-saving, and environment-friendly paper-based humidity sensor for multifunctional applications," *ACS applied materials & interfaces,* vol. 11, no. 24, pp. 21840-21849, 2019.

[52] X. Yu, Z. Wang, Y. Jiang *et al.*, "Reversible pH-responsive surface: From superhydrophobicity to superhydrophilicity," *Advanced Materials,* vol. 17, no. 10, pp. 1289-1293, 2005.

[53] J. Dong, and G. Portale, "Role of the Processing Solvent on the Electrical Conductivity of PEDOT:PSS," *Advanced Materials Interfaces,* vol. 7, no. 18, pp. 2000641, 2020.

[54] Y. H. Kim, C. Sachse, M. L. Machala *et al.*, "Highly Conductive PEDOT:PSS Electrode with Optimized Solvent and Thermal Post-Treatment for ITO-Free Organic Solar Cells," *Advanced Functional Materials,* vol. 21, no. 6, pp. 1076-1081, 2011.

[55] A. Beniwal, D. A. John, and R. Dahiya, "PEDOT:PSS-Based Disposable Humidity Sensor for Skin Moisture Monitoring," *IEEE Sensors Letters,* vol. 7, no. 3, pp. 1-4, 2023.

[56] A. Beniwal, P. Ganguly, R. Gond *et al.*, "Room Temperature Operated PEDOT: PSS Based Flexible and Disposable NO_2 Gas Sensor," *IEEE Sensors Letters*, pp. 1-4, 2023.

[57] T. Abel, B. Ungerböck, I. Klimant *et al.*, "Fast responsive, optical trace level ammonia sensor for environmental monitoring," *Chemistry Central Journal,* vol. 6, no. 1, pp. 124, 2012.

[58] S. Pandey, and K. K. Nanda, "Au Nanocomposite Based Chemiresistive Ammonia Sensor for Health Monitoring," *ACS Sensors,* vol. 1, no. 1, pp. 55-62, 2016.

[59] D. Ju, J. Kim, H. Yook *et al.*, "Engineering counter-ion-induced disorder of a highly doped conjugated polymer for high thermoelectric performance," *Nano Energy,* vol. 90, pp. 106604, 2021.

[60] A. Beniwal, P. Ganguly, D. K. Neethipathi *et al.*, "PEDOT:PSS modified Screen Printed Graphene-Carbon Ink based Flexible Humidity Sensor." *2022 IEEE International Conference on Flexible and Printable Sensors and Systems (FLEPS)*, Vienna, Austria, pp. 1-4, 2022.

[61] R. Sarabia-Riquelme, W. C. Schimpf, D. L. Kuhn *et al.*, "Influence of relative humidity on the structure, swelling and electrical conductivity of PEDOT:PSS fibers," *Synthetic Metals,* vol. 297, pp. 117399, 2023.

[62] S. A. Khan, M. Saqib, M. Khan *et al.*, "Wide-Range, Fast-Responsive Humidity Sensor Based on In_2Se_3/PEDOT:PSS Nanocomposite," *ACS Applied Electronic Materials,* vol. 5, no. 8, pp. 4473-4484, 2023.

[63] R. Sarabia-Riquelme, M. Shahi, J. W. Brill *et al.*, "Effect of Drawing on the Electrical, Thermoelectrical, and Mechanical Properties of Wet-Spun PEDOT:PSS Fibers," *ACS Applied Polymer Materials,* vol. 1, no. 8, pp. 2157-2167, 2019.

[64] Y. Seekaew, S. Lokavee, D. Phokharatkul *et al.*, "Low-cost and flexible printed graphene–PEDOT:PSS gas sensor for ammonia detection," *Organic Electronics,* vol. 15, no. 11, pp. 2971-2981, 2014.

[65] A. Marutaphan, Y. Seekaew, and C. Wongchoosuk, "Self-Consistent Charge Density Functional Tight-Binding Study of Poly(3,4-ethylenedioxythiophene): Poly(styrenesulfonate) Ammonia Gas Sensor," *Nanoscale Research Letters,* vol. 12, no. 1, pp. 90, 2017.

[66] A. Assadi, A. Spetz, M. Willander *et al.*, "Interaction of planar polymer Schottky barrier diodes with gaseous substances" *Sensors and Actuators B: Chemical* vol. 20, no. 1, pp 71-77, 1994.

[67] A. John, L. Benny, A. R. Cherian *et al.*, "Electrochemical sensors using conducting polymer/noble metal nanoparticle nanocomposites for the detection of various analytes: a review," *Journal of Nanostructure in Chemistry*, vol. 11, pp. 1-31 2021.

[68] C.-H. Hsieh, C.-H. Huang, P.-L. Chu, S.-Y. Chu, and P. Chen, "Investigation of the mechanism of a facile method for ammonia treatment to effectively tune the morphology and conductivity of PEDOT:PSS films," *Organic Electronics*, vol. 91, p. 106081, 2021.

Ajay Beniwal is presently working as a Marie Curie Fellow (Postdoctoral) in the James Watt School of Engineering, University of Glasgow, UK. He holds the prestigious Marie Skłodowska-Curie Postdoctoral Fellowships (UKRI funded). Before joining the current position, he served as Marie Curie Researcher/Post Doctoral Fellow at University of Glasgow, UK. Moreover, he received his PhD degree from the Department of Electronics and Communication Engineering, Indian Institute of Information Technology (IIIT), Allahabad, Prayagraj, India in 2021. He has been awarded the University Gold Medal during his Master's degree. He has authored and co-authored more than 29 publications in several prestigious journals and conferences. His current research interest includes sustainable electronic sensor devices, material characterization and thin film technology, printed and flexible electronics, for healthcare and agriculture applications.

Priyanka Ganguly is a Faculty at London Metropolitan University. She received her PhD in Nanotechnology from the Atlantic Technological University Sligo, Ireland, in 2021 and later spent her postdoctoral time at the University of Glasgow as a Marie Curie researcher. Priyanka has authored and co-authored more than 40 research articles and presented in several international and national conferences. She is the recipient of the Institute of Chemistry of Ireland Postgraduate Award in 2020 and Kathleen Longsdale Chemistry RIA prize of 2022.

Gaurav Khandelwal is currently working as a post-doctoral fellow in the Electronics and Nanoscale Engineering Division, University of Glasgow, UK. He completed his Ph.D. (with excellence) from the Department of Mechatronics Engineering at Jeju National University, South Korea, where he is a recipient of Brain Korea fellowship. His current research area includes triboelectric nanogenerators, piezoelectric nanogenerators, self-powered sensors, nanomaterial synthesis and characterisation.

Rahul Gond is a Ph.D. scholar at Department of Electrical Engineering, IIT Ropar, India. He received the B.Sc. and M.Sc. degrees in electronics and communication engineering from the University of Delhi, India, in 2017 and 2019, respectively. His current research interests include nanomaterial synthesis and characterization for environmental and bio-sensor applications, thin-film technology, printed and flexible electronics.

Brajesh Rawat received a B.Tech degree in Electronics and Communication Engineering from Rajiv Gandhi Proudyogiki Vishwavidyalaya, Bhopal, India in 2009. He obtained a PhD from the Indian Institute of Technology (IIT) Guwahati in 2018. From 2017 to 2018, he was a senior research fellow with the CENTD, IIT Guwahati. He works as an Assistant Professor in the Department of Electrical Engineering at IIT Ropar, India. He has authored and co- authored over 50 IEEE journal and conference research publications. His research interests include the fabrication and characterisation of chemical and biological sensors, and embedded system design.

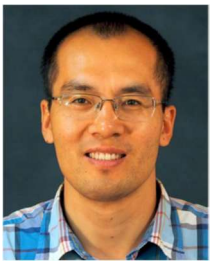

Chong Li (Senior Member, IEEE) was born in Liaoning, China, in 1979. He received the B.Eng. degree from Donghua University, Shanghai, China, in 2002, the M.Sc. degree (Hons.) from The University of Manchester, Manchester, U.K., in 2007, and the Ph.D. degree in electronics and electrical engineering from the University of Glasgow, Glasgow, U.K., in 2011. In 2011, he became a Post-Doctoral Research Assistant and later a Post-Doctoral Research Associate with the University of Glasgow, working on the development of millimeter-wave signal sources and terahertz imaging systems. In January 2014, he joined the National Physical Laboratory (NPL), Teddington, U.K., as a Higher Research Scientist. He became a Lecturer with the University of Glasgow, in 2017, a Senior Lecturer, in 2021 and a Professor, in 2023. He is currently leading the Microwave and Terahertz Electronics Research Group. His current research interests include semiconductor devices, microwave and terahertz components, and metrology.